SPECIAL ISSUE

CSIRO PUBLISHING

Environ. Chem. **2012**, *9*, 211–220
http://dx.doi.org/10.1071/EN11162

Research Paper

Characterisation of lightly oxidised organic aerosol formed from the photochemical aging of diesel exhaust particles

Jesse H. Kroll,[A,B,F] *Jared D. Smith,*[C,E] *Douglas R. Worsnop*[D] *and Kevin R. Wilson*[C]

[A]Department of Civil and Environmental Engineering, Massachusetts Institute of Technology, Cambridge, MA 02139, USA.
[B]Department of Chemical Engineering, Massachusetts Institute of Technology, Cambridge, MA 02139, USA.
[C]Chemical Sciences Division, Lawrence Berkeley National Laboratory, Berkeley, CA 94720, USA.
[D]Center for Aerosol and Cloud Chemistry, Aerodyne Research Inc., Billerica, MA 01821, USA.
[E]Present address: L. J. Smith and Associates, Rogers, AR 72756, USA.
[F]Corresponding author. Email: jhkroll@mit.edu

Environmental context. The effects of atmospheric fine particulate matter (aerosols) on climate and human health can be strongly influenced by the chemical transformations that the particles undergo in the atmosphere, but these 'aging' reactions are poorly understood. Here diesel exhaust particles are aged in the laboratory to better understand how they could evolve in the atmosphere, and subtle but unmistakable changes in their chemical composition are found. These results provide a more complete picture of the atmospheric evolution of aerosols for inclusion in atmospheric models.

Abstract. The oxidative aging of the semivolatile fraction of diesel exhaust aerosol is studied in order to better understand the influence of oxidation reactions on particle chemical composition. Exhaust is sampled from an idling diesel truck, sent through a denuder to remove gas-phase species and oxidised by hydroxyl ($OH^{\bullet}$) radicals in a flow reactor. $OH^{\bullet}$ concentrations are chosen to approximately match the $OH^{\bullet}$ exposures a particle would experience over its atmospheric lifetime. Evolving particle composition is monitored using aerosol mass spectrometry in two different modes, electron impact ionisation (EI) for the measurement of elemental ratios and vacuum ultraviolet (VUV) photoionisation for the measurement of molecular components. Changes to mass spectra in both modes indicate major changes to particle composition over the range of $OH^{\bullet}$ exposures studied. The product aerosol is only lightly oxidised ($O/C < 0.3$), suggesting an intermediate oxidation state between primary organics and the highly oxidised organic aerosol observed in the atmosphere. These lightly oxidised organics appear to be composed of secondary organic aerosol from semivolatile species, as well as from heterogeneously oxidised particle-phase organics. Key chemical characteristics (elemental ratios, oxidation kinetics and mass spectrometric features) of the reaction system are examined in detail. Similarities between this laboratory-generated aerosol and 'hydrocarbon-like organic aerosol' (HOA) reported in ambient studies suggest that HOA might not be entirely primary in origin, as is commonly assumed, but rather might include a significant secondary component.

Received 17 December 2011, accepted 6 April 2012, published online 20 June 2012

Introduction

Recent work has shown that organic aerosol (OA) generated under standard laboratory conditions tends to be substantially less oxidised than ambient OA.[1–5] This difference strongly suggests that most laboratory studies – and therefore many model treatments – do not capture the full extent of oxidation that organics undergo in the atmosphere. Instead, ongoing oxidation in the atmosphere will result in continual changes to the composition, loading and properties of OA over its atmospheric lifetime (days to weeks). As a result, there is intense interest in better understanding the chemistry (kinetics, mechanism and products) of aerosol aging processes.[6,7]

Recent aging studies have focussed on the heterogeneous oxidation of OA particles by the hydroxyl ($OH^{\bullet}$) radical,[8–19] in order to better understand the rates and key chemical steps associated with the oxidative degradation of particulate organic compounds. In our previous work on this topic[15–19] we have focussed on the oxidation of single-component model aerosol systems, simplifying the analysis of the reaction kinetics and products. In these experiments the particles were exposed to very high $OH^{\bullet}$ concentrations (the equivalent of up to several weeks in the atmosphere) in order to probe how later-generation (oxidised) products may themselves age in the atmosphere. Although this intensive oxidation of single-component particles

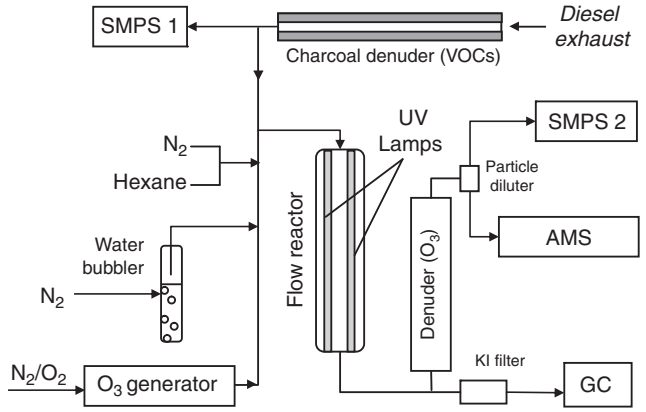

Fig. 1. The experimental setup (sample line, flow reactor and analytical instrumentation) used in this work. See text for details.

is useful for understanding key details of aging chemistry, these experimental conditions make it difficult to compare the aged OA in our experiments to that found in the atmosphere.

In this study we utilise our same general experimental approach to examine aerosol aging under more atmospherically relevant conditions. Rather than examine the chemistry of single model compounds, here we oxidise diesel exhaust aerosol, a highly complex mixture of reduced organics. Diesel exhaust includes high concentrations of gas-phase species – volatile organic compounds (VOCs) and intermediate-volatility organic compounds (IVOCs) – which have been shown to form secondary organic aerosol (SOA) very efficiently upon oxidation.[6,20] In order to probe the oxidative chemistry of only the lowest-volatility components of the aerosol, we therefore remove these gas-phase species before oxidation. Furthermore, these experiments utilise a much more modest range of $OH^{\bullet}$ exposures than in our previous studies, allowing us to study only those oxidative transformations that may occur over the atmospheric lifetime of the OA.

Experimental

The experimental setup used for this study is shown in Fig. 1. With the exception of the inlet for sampling diesel exhaust, this setup is identical to the one used in our previous experiments of the heterogeneous oxidation of model organic compounds, and is described only briefly here. Experiments were carried out at the Advanced Light Source (ALS) at Lawrence Berkeley National Laboratory, Berkeley CA. Diesel exhaust was sampled directly from the tailpipe of an idling truck (2000 Dodge Ram 3500) located just outside the laboratory. The vehicle, which runs on NA1993 ultra-low sulfur diesel and has no specific emissions control technology, was run in idling mode only; the effect of higher engine loads (which generally involve lower emissions of organics[21]) was not investigated in this study. The sampling inlet (a 3/8″ (0.95-cm) copper tube) was located ~5 cm from the tailpipe. The exhaust was then pulled at 1.3 L min^{-1} into the laboratory through a 3/8″ (0.95-cm) diameter, ~10 m-long unheated tube to our experimental setup.

Exhaust was first sent through a 1 m-long annular charcoal denuder to remove gas-phase species. (Losses of particles and low-volatility gas-phase organics may occur in the sampling line as well.) A fraction of the flow was sent into a scanning mobility particle sizer (SMPS, TSI Inc., Shoreview, MN) to monitor the concentration and size distribution of the sampled particles. Surface-weighted mean diameters of the particles were ~125–145 nm, with particle mass concentrations varying from 400 to 1000 μg m^{-3}.

The remainder of the diesel exhaust flow was sent into a flow reactor, a quartz flow tube with a length of 130 cm, inner diameter of 2.5 cm, and residence time of ~37 s. Oxidation was initiated by $OH^{\bullet}$ radicals, generated by the photolysis of ozone in the presence of water. This required that additional flows were added to the aerosol flow before the reactor. These flows included humidified nitrogen (relative humidity of 30 %), oxygen and ozone (generated from a corona discharge ozone generator). Together these flows dilute the aerosol flow by less than 50 %. Within the flow tube, ozone was photolysed by 254 nm light from two mercury lamps positioned just outside the quartz tube; these lamps also heated the tube somewhat, up to a temperature of ~35 °C. O_3 photolysis generated $O(^1D)$, which reacted with water vapour to form $OH^{\bullet}$. A trace amount of hexane (~100 ppb) was added to the tube, and measured using gas chromatography–flame ionisation detection (GC-FID) to quantify $OH^{\bullet}$ exposure.[15] $OH^{\bullet}$ concentrations, controlled by varying the concentration of O_3, ranged from $\sim 1.1 \times 10^9$ to 8×10^{10} molecule cm^{-3}. The resulting $OH^{\bullet}$ exposures corresponded to the equivalent of 4 h to 11 days in the atmosphere, assuming an average ambient $OH^{\bullet}$ concentration of 3×10^6 molecule cm^{-3} (although chemistry occurring over such short reaction times probably cannot be so simply extrapolated to atmospheric conditions[14,17]). Higher levels of $OH^{\bullet}$ in the flow tube have been accessed in our previous studies, but the focus of this work was on the initial oxidation of the diesel exhaust only. Nitrogen oxides (not measured in this experiment) in the exhaust might modify the subsequent oxidation chemistry somewhat, specifically by the reaction of NO with RO_2; however, we expect this reaction to be of minor importance due to the suppression of NO by the high concentrations of O_3 and HO_2.

The composition and size of particles exiting the flow reactor were measured using a high-resolution time-of-flight aerosol mass spectrometer (HR-ToF-AMS, Aerodyne Research, Inc., Billerica, MA), as well as a second SMPS (TSI Inc.). The AMS was modified to allow for two modes of ionisation of the aerosol components, electron impact ionisation (EI, the standard AMS approach), and vacuum ultraviolet photoionisation (VUV).[22] For EI, the vaporiser temperature was set to 600 °C, and the mass spectrum (using W-mode) and vacuum aerodynamic diameter (using V-mode) were measured. The high resolution of the mass spectrometer enables the determination of elemental ratios (O/C and H/C), using the approach of Aiken et al.[23,24] For VUV mode, radiation from the Chemical Dynamics Beamline (Beamline 9.0.2) of the ALS was used to photoionise the organics within the ionisation region of the AMS. The low photon energy used (10.5 eV) minimised ion fragmentation, allowing for improved identification of aerosol components.[25–27] We note that even when produced by VUV ionisation, oxygen-containing organic ions tend to fragment considerably,[15] precluding the molecular identification of the product species. Because of the lower sensitivity associated with photoionisation, for VUV measurements the AMS was run in V-mode only, with no particle sizing. For such measurements the vaporiser temperature was set to 100 °C, in order to minimise thermal energy imparted to the ions (which also contributes to fragmentation[28]). Thus the diesel oxidation experiments were carried out twice, first with the AMS in EI mode at 600 °C and then with the AMS in VUV mode at 100 °C. At this lower temperature there was significant organic signal in the 'closed' mode of the AMS (when the aerosol beam is blocked),

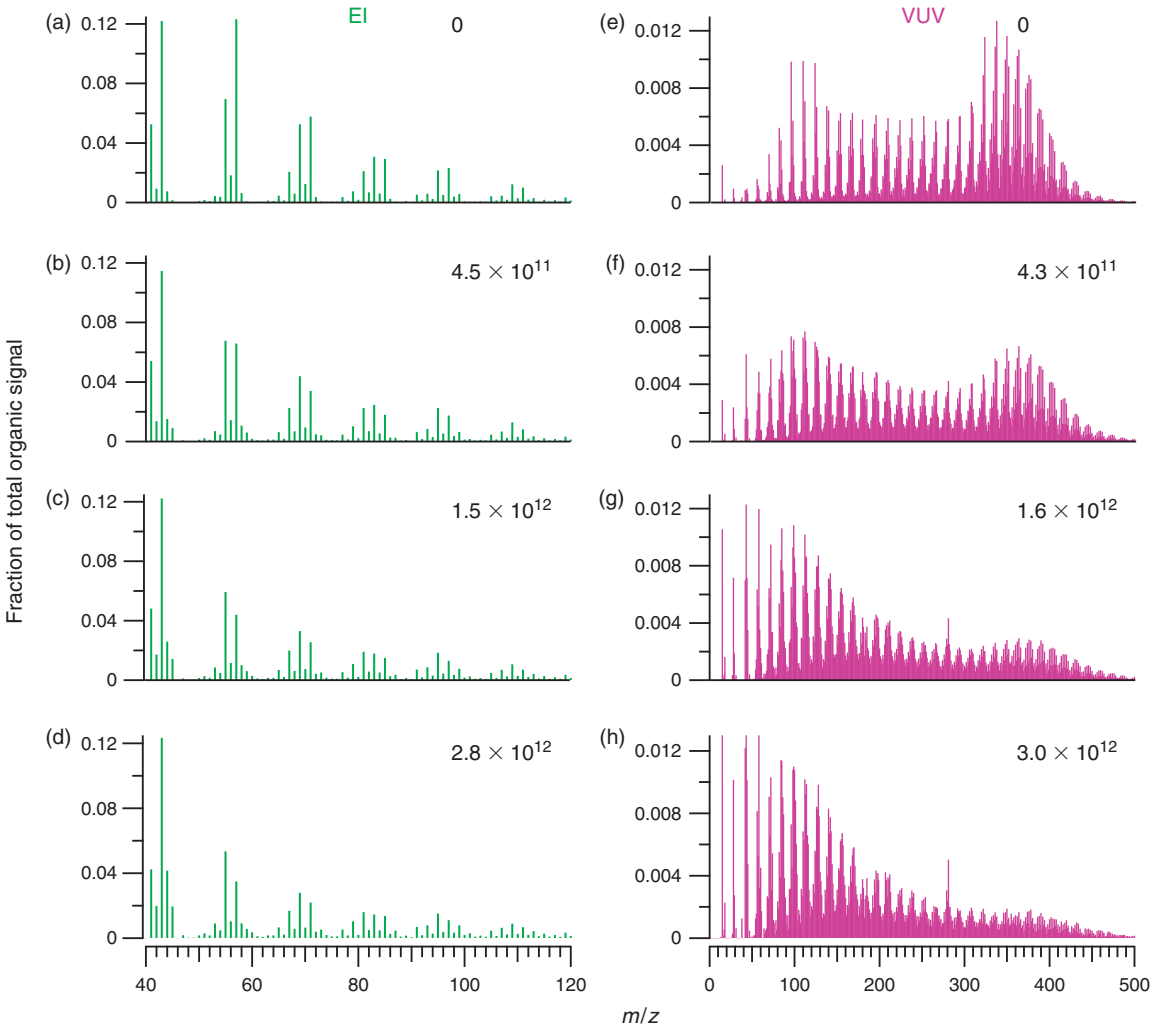

Fig. 2. Mass spectra (shown in unit-mass resolution) of diesel exhaust particles at different levels of oxidation. The top panels (a and e) correspond to unreacted diesel exhaust; lower panels correspond to particles after exposure to different $OH^{\bullet}$ levels ($OH^{\bullet}$ exposures are provided in each panel, molecule cm^{-3} s). Left panels (a–d): electron impact ionisation (EI) mass spectra. Right panels (e–h): vacuum ultraviolet photoionisation (VUV) mass spectra. The peak at *m*/*z* 281 corresponds to a siloxane impurity, as confirmed by high-resolution analysis.

suggesting relatively slow vaporisation. As a result, all reported VUV mass spectra are from running in 'open' mode only (as opposed to the standard 'difference' mode).

The combined SMPS/AMS measurements allowed particle mass to be determined, by the multiplication of average particle volume (from the SMPS) by the effective particle density. This in turn was computed from the ratio of vacuum aerodynamic diameter (as measured by the AMS in particle-time-of-flight mode) to mobility diameter (as measured by the SMPS).[29] This calculation assumed the particles were spherical, which is not strictly true due to the likely presence of elemental carbon (EC) in the particles.[21] However, as the particles were rich in aliphatic organics they were unlikely to be highly irregular in shape, and so the presence of EC was not expected to introduce significant errors in the particle mass calculation.[29]

Results

Evolving mass spectra

Fig. 2 shows normalised unit-mass-resolution (UMR) EI and VUV mass spectra for unreacted diesel exhaust, as well as exhaust exposed to differing levels of $OH^{\bullet}$. With the exception of changes in ozone concentrations (which control $OH^{\bullet}$ exposure) and drifts in the sampled particle number concentrations, reaction conditions (flows, irradiation by the mercury lamps, relative humidity, temperature, etc.) are held constant over all experiments. The mass spectra of the particles undergo marked changes with oxidation, indicating that the low-volatility (particulate) fraction of the diesel exhaust is subject to chemical changes over its atmospheric lifetime.

The EI spectra (Fig. 2a–d) are dominated by low-mass ions, due to the high degree of ion fragmentation associated with this ionisation technique. Changes in the EI spectra with oxidation involve shifts in the relative intensities of the different ion masses, including: (1) the increasing intensity of ions at *m*/*z* 44 and 45; (2) the decreasing intensity of higher-mass ions ($m/z > 45$) and (3) shifts in the relative intensities within each ion 'cluster' (e.g. *m*/*z* 40–45, 53–59, 65–73, etc.). These first two changes, which are necessarily related, are observed regularly in AMS studies, with *m*/*z* 44 being a major indicator of organic acids and related species.[30] At the same time, none of these spectra appear to have reached the high degree of oxidation of

'oxidised organic aerosol' (OOA) observed in ambient conditions.[7,24,31] This suggests that over these $OH^{\bullet}$ exposures, these experiments are accessing an intermediate oxidation state, forming particulate organics that are only lightly oxidised. The third change to the spectra, which involves a shift to lower 'delta series' of the ions,[1,32] reflects more subtle shifts in particle composition, and is discussed in a later section.

The VUV mass spectra (Fig. 2e–h) exhibit high ion intensities over a much wider range of masses, as expected for this soft ionisation technique. The high-mass mode (right side of each spectrum, m/z 300–500) corresponds mostly to molecular ions, which have masses corresponding to aliphatic hydrocarbons (21–36 carbon atoms per molecule). The most intense peak in the mass spectrum of the unoxidised exhaust aerosol is at 338.39, corresponding to $C_{24}H_{50}$. The lower-mass peaks ($m/z < 300$) are likely to be dominated by fragment ions. When viewed in high-resolution, all major peaks exhibit large positive mass defects (with exact masses substantially above their integer values), indicating high hydrogen content; this confirms the dominance of aliphatic organics in the exhaust. Peaks corresponding to hydrogen-poor polycyclic aromatic hydrocarbons (e.g. $C_{20}H_{12}^{+}$, m/z 252.09, corresponding to benzo[a]pyrene) are also observed, but these are very small compared with their corresponding aliphatic isobaric ions (e.g. $C_{18}H_{36}^{+}$, m/z 252.28). Thus polycyclic aromatic hydrocarbons likely represent a minor component of the particles, consistent with results from previous studies.[33]

The VUV aerosol mass spectrum changes much more dramatically upon oxidation than does the EI spectrum, with a rapid decrease in the intensity of the high-mass mode (molecular ions) and a corresponding increase in the lower-mass peaks (fragment ions). This is because oxygen-containing species fragment much more readily upon VUV photoionisation than do reduced species; thus as the aerosol becomes more oxidised, the degree of ion fragmentation increases, leading to the large observed shifts in the VUV mass spectra.

Changes in elemental composition of the organics

The high resolution of the EI mass spectra enables the determination of elemental ratios of the particulate organics,[23,24] most importantly the hydrogen-to-carbon ratio (H/C) and the oxygen-to-carbon ratio (O/C). Fig. 3a shows the evolving elemental ratios of the organic particulate matter in a 'van Krevelen plot', a plot of H/C *v*. O/C. As has been seen in other aliphatic systems,[4] the unoxidised (primary) particles begin in the top left of the plot (H/C = 2.06, O/C = 0.025), and move down and to the right upon oxidation. However, even at the highest levels of oxidation accessed in these experiments, the particles are not as oxidised as most ambient OOA fractions,[4,34] again suggesting the resulting particles are in their early stages of oxidation.

Two distinct slopes in Krevelen space are seen. At low levels of oxidation (O/C < 0.1), the data follow a slope of −1.93; this is close to the −2 slope associated with the introduction of carbonyl (ketone or aldehyde) functional groups to the condensed-phase organics, suggesting the importance of these moieties in the early stages of oxidation. At higher levels of oxidation, the data instead follow a shallower slope of −0.93, close to the slope of −1 associated with addition of carboxylic acid or hydroxycarbonyl functionalities. This shift in the van Krevelen slope, and therefore in the formation of particle-phase products, is very similar to what we observed in our previous study of the heterogeneous oxidation of squalane.[4,16] We note that these changes in the elemental ratios result solely from oxidative aging of the aerosol; therefore observations of similar slopes under ambient conditions may reflect aging chemistry and cannot necessarily be attributed solely to physical (e.g. mixing) processes.[4,34] Results from other laboratory and field studies show that at even higher levels of oxidation, the slope appears to level off still further, to values of −0.5,[4,34] reflecting yet another shift in the aging chemistry for more highly oxidised species.

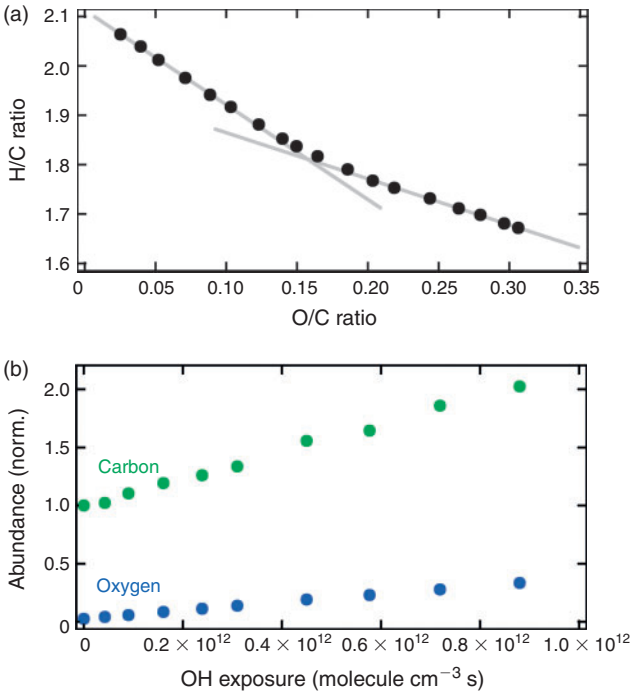

Fig. 3. Evolving elemental composition of the diesel exhaust particles. (a) van Krevelen plot, with oxidation involving movement down and to the right. The trajectories follow two slopes, first −1.93 then −0.93. Both linear fits (determined from the six least-oxidised and the seven most-oxidised data points respectively) are shown. (b) abundances of particulate carbon (green) and oxygen (blue) in the particles, normalised to the amount of carbon in the unreacted system, as a function of $OH^{\bullet}$ exposure.[16] The increase in carbon abundance indicates the formation of secondary organic aerosol, presumably from gas-phase semivolatile organics.

We have previously demonstrated the utility of examining aging chemistry using not only elemental ratios (O/C and H/C) but also elemental abundances (the amount of carbon, hydrogen and oxygen in the particle phase). In our earlier study of the heterogeneous oxidation of squalane,[16] the calculation of elemental abundances allowed for the determination of the relative importance of two key oxidation channels, functionalisation (the addition of oxygen-containing functional groups to a carbon skeleton) and fragmentation (the breaking of the carbon skeleton).[16] Here we calculate elemental abundances of the diesel exhaust particles from particle mass and elemental ratios, using the same approach as in that study.[16] To account for possible changes in the amount of exhaust sampled into the tube, elemental abundances are corrected for changes to particle number concentration, as measured by the first SMPS (located upstream of the flow reactor).

Fig. 3b shows the elemental abundances of carbon and oxygen as functions of $OH^{\bullet}$ exposure. As expected, the oxygen

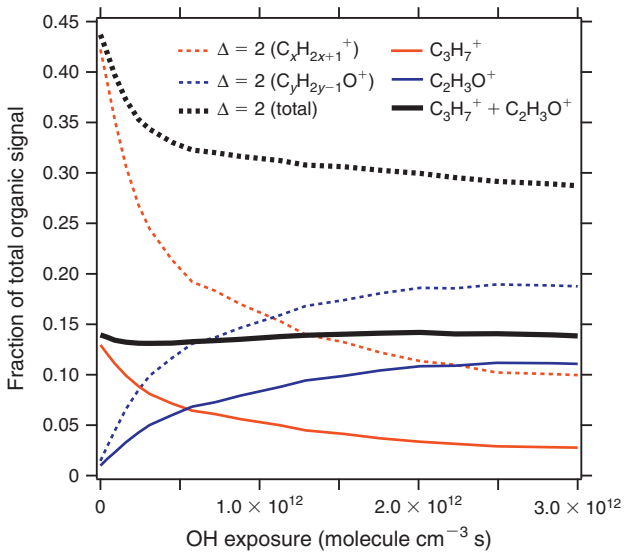

Fig. 4. Normalised electron impact ionisation (EI) signal (ion intensity as a fraction of total) of the *m/z* 43 ions (solid lines) and all ions in the $\Delta = +2$ series (dotted lines). Changes to individual ions, as determined at high resolution, are much more dramatic than at a given nominal mass, due to the simultaneous decrease in $C_xH_{2x+1}^+$ signal and increase in ($C_yH_{2y-1}O^+$) signal.

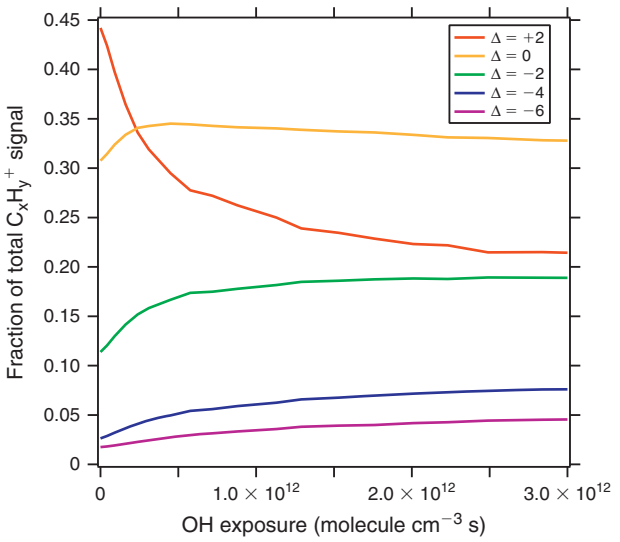

Fig. 5. Evolution of the hydrocarbon ions (of form $C_xH_y^+$) in the electron impact ionisation (EI) mass spectra. Contributions of $C_xH_y^+$ ions in each delta series, as a fraction of the total $C_xH_y^+$ signal, are plotted against OH$^\bullet$ exposure. As oxidation increases, the $\Delta = +2$ series gives way to $\Delta = 0$, as well as to $\Delta = -2$, -4, and -6. These lower Δ-series hydrocarbon ions are likely derived from oxidised organics, which may lose oxygen during vaporisation or ionisation within the aerosol mass spectrometer.

content increases at higher levels of OH$^\bullet$. In addition, carbon content also increases; this is in marked contrast to the heterogeneous oxidation of squalane[16] (as well as of other model organic species[18]), which exhibits decreases in carbon content due to fragmentation reactions. This new particulate carbon provides strong evidence for the formation of SOA, from the oxidation of gas-phase organics followed by gas-to-particle conversion. Indeed, at all but the lowest OH$^\bullet$ exposures, the SMPS detects a nucleation mode; this new mode contributes negligibly to particle mass but provides unambiguous evidence for SOA formation. At higher OH$^\bullet$ exposures (not shown), the increased mass from SOA drops rather abruptly, although it does not disappear entirely; it is unclear whether this drop is related to a change in the engine output or is a real chemical effect. In any case, the charcoal denuder between the sample inlet and the flow reactor, intended to scavenge all gas-phase SOA precursors, clearly does not prevent the presence of gas-phase organics in the flow tube. This may be due to evaporation of semivolatile material downstream of the denuder, possibly promoted by heating of the flow reactor by the mercury lamps.

Changes in relative ion intensities in the EI mass spectra

As shown in Fig. 2, the relative intensities of ions of different nominal masses within each 'cluster' of the EI spectra change upon oxidation, with increased oxidation leading to decreases in higher-mass ions and increases in the lower-mass ions. This evolution can be described in terms of the ion (or 'delta') series approach, which classifies organics in an EI mass spectrum by grouping ions that differ by 14 mass units (corresponding to the addition or subtraction of CH_2).[1,32] In this approach, each series is assigned a 'delta value' (Δ) equal to $m/z\ -14n + 1$, where n is an integer nominally equal to the number of CH_2 groups in the ion. In the system studied here, the mass spectrum of unoxidised diesel exhaust particles (Fig. 2a) is dominated by the $\Delta = +2$ series, which consists of ions at *m/z* 29, 43, 57, 71, etc. As OH$^\bullet$ levels increase, these $\Delta = +2$ ions give way to ions in the $\Delta = 0$ series (*m/z* 41, 55, 69…) and the $\Delta = -2$ series (*m/z* 39, 53, 67…). Such changes are examined in more detail in Figs 4 and 5.

Fig. 4 shows changes to the fractional contribution of *m/z* 43, as well as its delta series ($\Delta = +2$), to total EI signal. At unit mass resolution, the *m/z* 43 fraction (heavy black curve) is approximately constant with OH$^\bullet$ exposure (at ~13 % of total ion signal). However, examination of the high-resolution mass spectrum shows that the two ions that dominate the signal at this nominal mass, $C_3H_7^+$ (*m/z* 43.055) and $C_2H_3O^+$ (*m/z* 43.018), change dramatically over this range of OH$^\bullet$ exposures. The $C_3H_7^+$ ion, which accounts for virtually all the *m/z* 43 signal in the unoxidised particles, quickly drops with OH$^\bullet$ exposure (solid red curve), whereas the $C_2H_3O^+$ (solid blue curve) grows in; these changes approximately cancel each other out, leading to the constant *m/z* 43 fraction. The entire $\Delta = +2$ series (*m/z* 43, 57, 71, 85…), shown as dotted curves in Fig. 4, behaves similarly, with a decrease in the $C_xH_{2x+1}^+$ fraction counterbalanced by an increase in the $C_yH_{2y-1}O^+$ fraction. However, for the larger mass ions, the two changes do not completely cancel, leading to an overall decrease in the fractional intensity of the $\Delta = +2$ series as a whole. These results point to the importance of isobaric ions (which differ in the number of oxygen atoms) in the oxidative evolution of organic particles, and highlight the utility of high-resolution mass spectrometry for understanding the mechanisms of aerosol aging.

However, this shift to more oxygenated ions does not explain all the changes in the relative ion intensities seen in the EI spectra. Shown in Fig. 5 are the evolving fractional contributions of each $C_xH_y^+$ delta series to the total $C_xH_y^+$ signal. Even though all the species included are nominally hydrocarbon ions, their relative intensities vary dramatically with oxidation. The hydrocarbon ions in the $\Delta = +2$ series ($C_xH_{2x+1}^+$ ions: $C_2H_5^+$, $C_3H_7^+$, $C_4H_9^+$…) are the major ions in unoxidised diesel exhaust, accounting for almost half the total ion signal. However, this fraction drops rapidly with oxidation, in favour of the lower

delta series. After only minimal oxidation, the $\Delta = 0$ hydrocarbon ions ($C_xH_{2x-1}^+$ ions: $C_2H_3^+$, $C_3H_5^+$, $C_4H_7^+$ …) emerge as the major contributors to the $C_xH_y^+$ signal; however, upon further oxidation even these ions become less dominant, as still lower delta series ions ($\Delta = -2$, -4, and -6) increase in importance throughout. (The odd-numbered delta series, corresponding to the even-mass ions, tend to be minor and do not exhibit any significant trend.) These lower-Δ ions are generally associated with unsaturated hydrocarbons such as alkenes and cycloalkanes[32]; however, it seems unlikely the relative abundances of such molecules would increase with $OH^\bullet$ exposure. Instead we believe these ions are formed from oxygenates, as a result of oxygen loss either on the vaporiser (by thermal or pyrolytic decomposition) or in the ionisation region (by neutral loss) in the AMS. Such processes will likely lead to the formation of unsaturated (low-Δ) ions, as is observed. Indeed, the lower hydrogen number of the lower-Δ ions indicates a higher carbon oxidation state,[5] and thus it is expected that such ions will increase in abundance at higher $OH^\bullet$ exposures.

Kinetics and products of oxidative aging

An accurate picture of aerosol aging requires an understanding of the rate of the aging reactions as well as of the key chemical properties of the aging products. In our previous studies of the oxidation of single-component model organic particles, it was relatively straightforward to estimate such quantities, by tracking the concentration of the reactant species (usually using a single marker ion in the mass spectrum), and measuring the aerosol composition after depletion of the reactant species.[15,18] This approach cannot be used for the present studies, as diesel exhaust aerosol involves (at least) hundreds of individual species, precluding the use of individual marker ions.

Instead we utilise a spectral subtraction approach, similar to that used by Sage et al.,[35] in which the unreacted diesel exhaust mass spectrum is scaled and subtracted from the mass spectrum of the oxidised aerosol. The largest scaling factor for which no peaks become negative gives an upper limit to the fraction of unreacted organics still present in the particle. All spectra used were normalised to total ion signal; because particle mass increases due to SOA condensation, this normalisation may lead to an oversubtraction, and hence an underestimate (by up to a factor of ~2) of the fraction of unreacted organics remaining. This spectral subtraction approach was applied to both the high-resolution EI spectra (m/z 12–120) and the unit-mass-resolution VUV spectra (m/z 40–600). Results (fraction of unreacted diesel exhaust remaining *v*. $OH^\bullet$ exposure) are shown in Fig. 6. The fractional loss of the unreacted organics is substantial, exceeding 90 % at the highest $OH^\bullet$ exposures studied. As this fractional decrease is much larger than the fractional increase of particle mass by SOA condensation (Fig. 3b), the unreacted organics are being lost in an absolute sense, rather than simply being diluted by the additional SOA mass. This indicates that the initial aerosol components themselves are undergoing oxidation, which (along with SOA formation) will affect the chemical composition of the particles. Some of this oxidation may occur in the gas phase, by evaporation–oxidation–recondensation of semivolatile species (the 'semivolatile pumping' mechanism[36]). However, the residence time in the flow reactor (37 s) may be too short to allow for full semivolatile equilibrium partitioning; thus, the heterogeneous oxidation of particulate organics by gas-phase $OH^\bullet$ is also likely to play a role in this degradation chemistry.

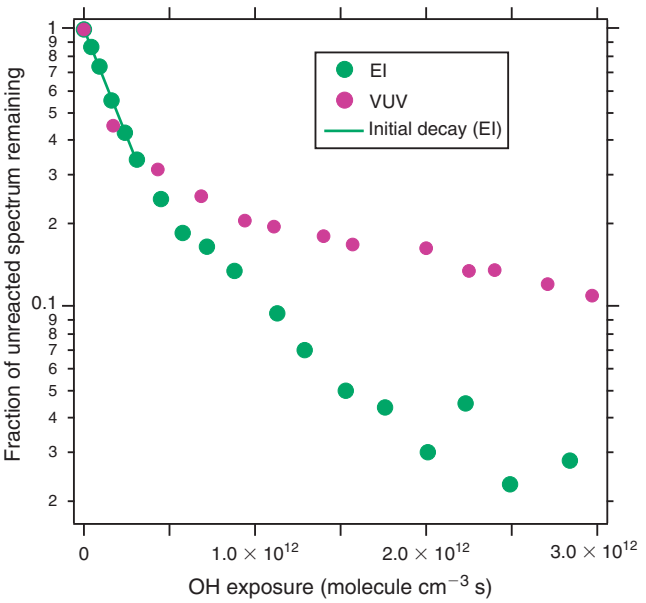

Fig. 6. Reactive loss of the particulate organics in diesel exhaust. The fraction of unreacted organics remaining in the particle, as calculated by spectral subtraction (see text), is plotted versus $OH^\bullet$ exposure, for both electron impact ionisation (EI) and vacuum ultraviolet photoionisation (VUV) data. The solid line is an exponential fit to the initial decay (EI data only), allowing for the determination of the reaction rate and effective uptake coefficient.

At low $OH^\bullet$ exposures ($\leq 3.1 \times 10^{11}$ molecule cm^{-3} s), the unreacted diesel exhaust decays exponentially, with a decay constant (determined from fitting the EI spectral subtraction results in this range) of 3.6×10^{-12} cm^3 $molecule^{-1}$ s^{-1}. (Only one VUV experiment was made in this $OH^\bullet$ exposure range, and is reasonably consistent with the EI results.) This decay constant corresponds to the second-order rate constant of the $OH^\bullet$-particle reaction ($k_{OH\bullet}$), and allows for the determination of the effective uptake coefficient ($\gamma_{OH\bullet}$), the ratio of the rate of reactive loss of the particulate organics to the $OH^\bullet$ collision rate with the particle surface.[15] The uptake coefficient is calculated from the rate using the expression:

$$\gamma_{OH^\bullet} = \frac{2D_0 \rho N_A}{3\bar{c}_{OH^\bullet} M} k_{OH^\bullet} \quad (1)$$

where D_0 is the surface-area-weighted mean particle diameter, ρ is the particle density, M is the average molecular weight of the particle (taken to be 338 g mol^{-1}, from Fig. 2e), N_A is Avogadro's number and $\bar{c}_{OH\bullet}$ is the mean speed of the hydroxyl radical. The uptake coefficient is calculated to be 0.9; this is higher than our measured values for squalane, but again is likely to be an upper limit, given the spectral subtraction approach used. Due to unknown amounts of secondary chain chemistry and uncertainty with regard to the 'semivolatile pumping' mechanism, this uptake coefficient is not explicitly corrected for gas-phase diffusion of $OH^\bullet$.[37] Regardless, this value of $\gamma_{OH\bullet}$ is substantially lower than those determined by Lambe et al. for individual semivolatile components within fuel or motor oil.[38] That study was carried out using an environmental chamber, and the high values of $\gamma_{OH\bullet}$ (often well above unity) were taken as evidence of evaporation followed by gas-phase oxidation. The much lower $\gamma_{OH\bullet}$ value determined in our study suggests that such a

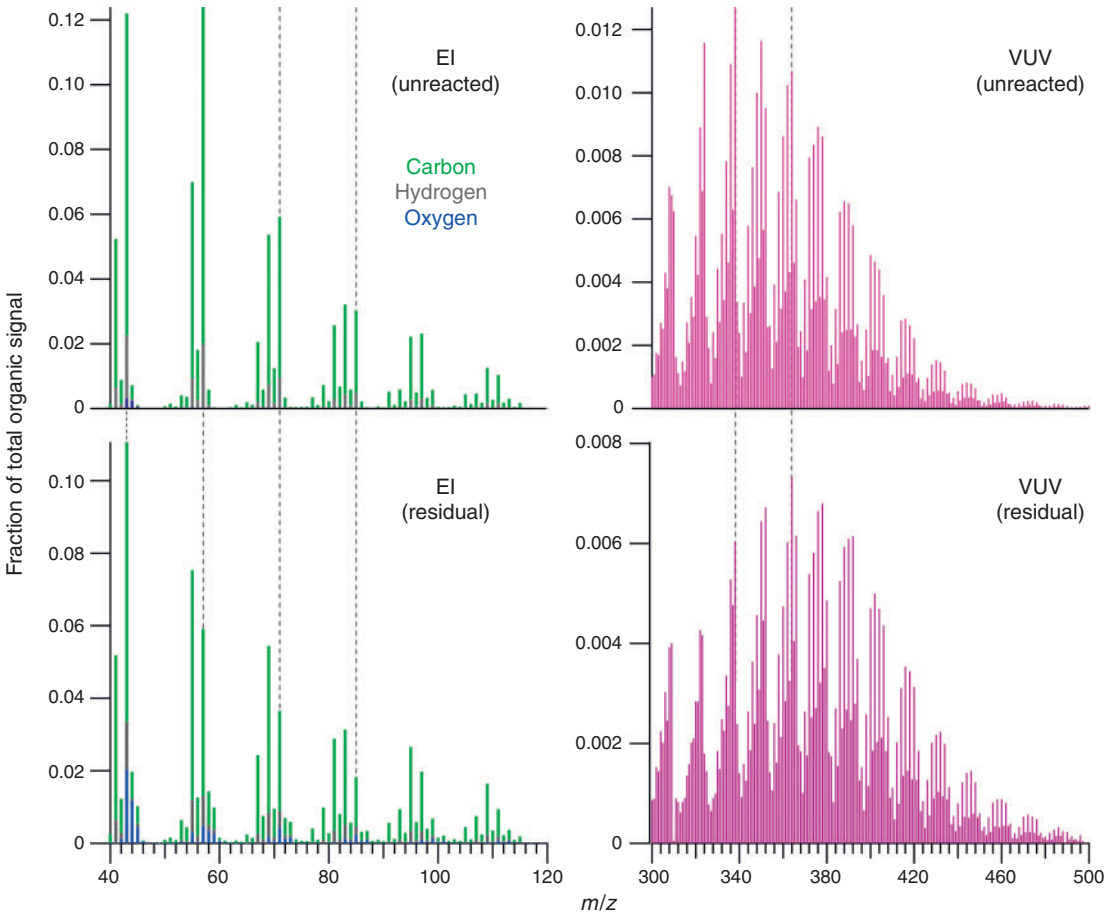

Fig. 7. Reactant and product mass spectra for the initial aging of diesel exhaust particles. Top panels: unreacted diesel exhaust particles in electron impact ionisation (EI) and vacuum ultraviolet photoionisation (VUV) spectra (same as Fig. 2a and 2e respectively). The EI spectra are coloured by the mass contribution of different elements at each nominal *m/z* value. Bottom panels: EI and VUV product mass spectra, determined from spectral subtraction of the unreacted spectra from the spectra of oxidised diesel exhaust particles, at the lowest level of $OH^{\bullet}$ exposure studied (4.3×10^{10} molecule cm^{-3} s for EI and 1.7×10^{11} molecule cm^{-3} s for VUV). Vertical dashed lines highlight key differences in the residual spectra: major $\Delta = +2$ masses (*m/z* 43, 57, 71 and 85) for EI, and the most intense molecular peaks (*m/z* 338 and 364) for VUV.

mechanism does not occur efficiently in our system. This may be a result of the prior removal of the most volatile components of the aerosol by the denuder, the high aerosol loadings used or the short timescales within our flow reactor, any of which could minimise the evaporation of semivolatile species.

At higher $OH^{\bullet}$ exposure levels, the decrease in the fraction of unreacted organics appears to slow down, as evidenced by the shallower slopes on the right side of Fig. 6. The reason for this apparent slowing of the chemistry is not clear. This shift occurs at approximately the same $OH^{\bullet}$ exposure as the change in the slope of the van Krevelen plot (Fig. 3a), suggesting it may be related to changes to the oxidation mechanism, but this is only speculative. It should also be noted that the EI and VUV spectral subtraction results diverge considerably at these high $OH^{\bullet}$ exposures. This may arise from the difference in selectivity of the two techniques. If the product spectra share many features with reactant spectra, then this spectral subtraction approach will overestimate the degree to which the reactant is lost. This effect will be most pronounced for the least selective techniques; as EI is relatively unselective, the inferred loss of unreacted organics is expected to be greater for EI than for VUV, as is observed here.

Shown in Fig. 7 are residual spectra, obtained by subtracting the mass spectrum of unreacted diesel exhaust (shown at top) from that of the oxidised aerosol at the lowest level of $OH^{\bullet}$ exposure studied (4.3×10^{10} molecule cm^{-3} s for EI and 1.7×10^{11} molecule cm^{-3} s for VUV). These spectra represent early generation oxidation products. For EI, the shifts in the ion intensities towards lower delta series are evident, and the elemental ratios associated with the residual aerosol (O/C = 0.15, H/C = 1.86) indicate the organics are mildly oxidised. In VUV the residual (product) spectrum exhibits a clear shift towards higher mass peaks, with the most intense ion at *m/z* 364 (up from *m/z* 338 for the unreacted diesel exhaust). This may indicate that the lighter molecules react away more rapidly than the heavier ones do. Interestingly, none of the molecular ions in the VUV residual spectrum appear to include oxygen atoms, in stark contrast with our results from heterogeneously oxidised squalane.[15] This suggests that the multiphase oxidation chemistry of diesel exhaust aerosol is fundamentally different than that in our previous studies; further study is required to determine whether this arises from differences in particle volatility, or from something more specific to the chemical components of diesel exhaust aerosol.

Discussion

In this work we have examined the oxidative aging of diesel exhaust particles, with a focus on (1) the chemistry of the lowest-volatility fraction of the OA (particulate organics and gas-phase semivolatiles) and (2) the initial stages of oxidation, before the formation of highly oxidised species. The evolution of the elemental ratios of the particulate organics (Fig. 3a) is found to be similar to that of the heterogeneous oxidation of squalane.[4,16] However, from the elemental abundances (Fig. 3b) it is clear that the aging pathway for diesel exhaust particles is quite different, involving major contributions by gas-phase oxidation (SOA formation). This underscores the utility of elemental abundances (and not just elemental ratios) for elucidating key processes in aerosol aging. Moreover, it suggests that disparate aging processes may result in products with similar elemental ratios – and hence properties[7,39] – which may help simplify the modelling of aerosol aging considerably.[4]

The aerosol formed in these experiments is only lightly oxidised, with an O/C (and carbon oxidation state) significantly lower than that of the OOA component of ambient aerosol. This is apparent in the EI spectra (Fig. 2a–d), which lack the intense signal at m/z 44 (CO_2^+) that characterises OOA. Thus this study confirms previous work (e.g. George and Abbatt,[13] DeCarlo et al.[40]) indicating that heterogeneous chemistry is too slow to contribute to OOA formation; it also suggests that SOA from the lowest-volatility component of diesel exhaust probably cannot form OOA either. In fact the product spectra look similar to the 'hydrocarbon-like organic aerosol' (HOA) fraction of ambient aerosol, consistent with a very recent SOA study using a similar reactor.[41] HOA is generally taken to be indicative of primary emissions; however, the EI spectra of the lightly oxidised particles (Fig. 2b–d) have some features that distinguish them from primary OA (Fig. 2a), such as elevated intensities of oxygen-containing ions and shifts towards ions with fewer hydrogen atoms (lower Δ-series). The dramatic changes to the VUV mass spectra (Fig. 2e–h) provide further evidence of the substantial transformation that the aerosol components undergo as a result of oxidation.

The reaction conditions within our flow reactor (e.g. high oxidant concentrations, high particle loadings, low reaction times, and irradiation at 254 nm) vary considerably from those of the atmosphere. Nonetheless there are some intriguing similarities between the EI spectra of the lightly oxidised aerosol generated in these studies and AMS spectra of ambient aerosol. Ambient HOA spectra tend to have elevated ion intensities at lower delta series ($\Delta = 0, -2$),[42] as well as higher O/C ratios (as high as 0.16),[24,43,44] relative to pure hydrocarbon mixtures (such as fuel and lubricating oil). Although these spectroscopic features may result from primary OA that includes some oxygen (from sources such as trash burning[45] or vehicles without aftertreatment devices[20]), they may also indicate early oxidative processing of the primary aerosol. Similarly, AMS measurements just downwind of the 2010 Gulf oil spill (R. Bahreini, A. M. Middlebrook, C. A. Brock, J. A. de Gouw, S. A. McKeen, L. R. Williams, K. E. Daumit, A. T. Lambe et al., unpubl. data) found that the OA was relatively unoxidised, with O/C ratios as low as 0.3, particularly in areas most influenced by IVOC (as opposed to VOC) emissions. Such aerosol (which is very likely to be secondary in nature[46]) provides strong evidence for the atmospheric formation of photochemically generated, lightly oxidised OA, similar to the aerosol generated in our flow reactor.

The present experiments indicate that low-volatility organic species, in the particle or gas phase, may oxidise to form mildly oxidised OA over relatively short atmospheric timescales (hours to days). Using the AMS, this aerosol looks quite similar to HOA, generally taken to be purely primary in nature; however, the constituent organics may actually be formed from atmospheric oxidation reactions. Thus much of the HOA reported in ambient studies may include a significant secondary (albeit lightly oxidised) component. The resulting aerosol will likely have somewhat different properties than pure primary OA, which may imply different effects on human health and climate. Future study of the composition, properties, and chemical signatures of such lightly oxidised organics will help clarify the atmospheric importance and effects of this class of organic particulate matter.

Acknowledgements

This work was supported in part by the Director, Office of Energy Research, Office of Basic Energy Sciences, Chemical Sciences Division of the US Department of Energy under contract number DE-AC02-05CH11231. J. D. Smith was supported by the Camille and Henry Dreyfus Foundation postdoctoral program in environmental chemistry.

References

[1] R. Bahreini, M. D. Keywood, N. L. Ng, V. Varutbangkul, S. Gao, R. C. Flagan, J. H. Seinfeld, D. R. Worsnop, J. L. Jimenez, Measurements of secondary organic aerosol from oxidation of cycloalkenes, terpenes, and *m*-xylene using an Aerodyne aerosol mass spectrometer *Environ. Sci. Technol.* **2005**, *39*, 5674. doi:10.1021/ES048061A

[2] P. S. Chhabra, R. C. Flagan, J. H. Seinfeld, Elemental analysis of chamber organic aerosol using an aerodyne high-resolution aerosol mass spectrometer. *Atmos. Chem. Phys.* **2010**, *10*, 4111. doi:10.5194/ACP-10-4111-2010

[3] P. S. Chhabra, N. L. Ng, M. R. Canagaratna, A. L. Corrigan, L. M. Russell, D. R. Worsnop, R. C. Flagan, J. H. Seinfeld, Elemental composition and oxidation of chamber organic aerosol. *Atmos. Chem. Phys.* **2011**, *11*, 8827. doi:10.5194/ACP-11-8827-2011

[4] C. L. Heald, J. H. Kroll, J. L. Jimenez, K. S. Docherty, P. F. DeCarlo, A. C. Aiken, Q. Chen, S. T. Martin, D. K. Farmer, P. Artaxo, A. J. Weinheimer, A simplified description of the evolution of organic aerosol composition in the atmosphere. *Geophys. Res. Lett.* **2010**, *37*, L08803. doi:10.1029/2010GL042737

[5] J. H. Kroll, N. M. Donahue, J. L. Jimenez, S. H. Kessler, M. R. Canagaratna, K. R. Wilson, K. E. Altieri, L. R. Mazzoleni, A. S. Wozniak, H. Bluhm, E. R. Mysak, J. D. Smith, C. E. Kolb, D. R. Worsnop, Carbon oxidation state as a metric for describing the chemistry of atmospheric organic aerosol. *Nat. Chem.* **2011**, *3*, 133. doi:10.1038/NCHEM.948

[6] A. L. Robinson, N. M. Donahue, M. K. Shrivastava, E. A. Weitkamp, A. M. Sage, A. P. Grieshop, T. E. Lane, J. R. Pierce, S. N. Pandis, Rethinking organic aerosols: semivolatile emissions and photochemical aging. *Science* **2007**, *315*, 1259. doi:10.1126/SCIENCE.1133061

[7] J. L. Jimenez, M. R. Canagaratna, N. M. Donahue, A. S. H. Prevot, Q. Zhang, J. H. Kroll, P. F. DeCarlo, J. D. Allan, H. Coe, N. L. Ng, A. C. Aiken, K. S. Docherty, I. M. Ulbrich, A. P. Grieshop, A. L. Robinson, J. Duplissy, J. D. Smith, K. R. Wilson, V. A. Lanz, C. Hueglin, Y. L. Sun, J. Tian, A. Laaksonen, T. Raatikainen, J. Rautiainen, P. Vaattovaara, M. Ehn, M. Kulmala, J. M. Tomlinson, D. R. Collins, M. J. Cubison, E. J. Dunlea, J. A. Huffman, T. B. Onasch, M. R. Alfarra, P. I. Williams, K. Bower, Y. Kondo, J. Schneider, F. Drewnick, S. Borrmann, S. Weimer, K. Demerjian, D. Salcedo, L. Cottrell, R. Griffin, A. Takami, T. Miyoshi, S. Hatakeyama, A. Shimono, J. Y. Sun, Y. M. Zhang, K. Dzepina, J. R. Kimmel, D. Sueper, J. T. Jayne, S. C. Herndon, A. M. Trimborn, L. R. Williams, E. C. Wood, A. M. Middlebrook, C. E. Kolb, U. Baltensperger, D. R. Worsnop, Evolution of organic aerosols in the atmosphere. *Science* **2009**, *326*, 1525. doi:10.1126/SCIENCE.1180353

[8] A. T. Lambe, J. Zhang, A. M. Sage, N. M. Donahue, Controlled OH radical production via ozone-alkene reactions for use in aerosol aging studies. *Environ. Sci. Technol.* **2007**, *41*, 2357. doi:10.1021/ES061878E

[9] I. L. George, A. Vlasenko, J. G. Slowik, K. Broekhuizen, J. P. D. Abbatt, Heterogeneous oxidation of saturated organic aerosols by hydroxyl radicals: uptake kinetics, condensed-phase products, and particle size change. *Atmos. Chem. Phys.* **2007**, *7*, 4187. doi:10.5194/ACP-7-4187-2007

[10] V. F. McNeill, R. L. N. Yatavelli, J. A. Thornton, C. B. Stipe, O. Landgrebe, Heterogeneous OH oxidation of palmitic acid in single component and internally mixed aerosol particles: vaporization and the role of particle phase. *Atmos. Chem. Phys.* **2008**, *8*, 5465. doi:10.5194/ACP-8-5465-2008

[11] I. J. George, J. Slowik, J. P. D. Abbatt, Chemical aging of ambient organic aerosol from heterogeneous reaction with hydroxyl radicals. *Geophys. Res. Lett.* **2008**, *35*, L13811. doi:10.1029/2008GL033884

[12] I. J. George, J. P. D. Abbatt, Chemical evolution of secondary organic aerosol from OH-initiated heterogeneous oxidation. *Atmos. Chem. Phys.* **2010**, *10*, 5551. doi:10.5194/ACP-10-5551-2010

[13] I. J. George, J. P. D. Abbatt, Heterogeneous oxidation of atmospheric aerosol particles by gas-phase radicals. *Nat. Chem.* **2010**, *2*, 713. doi:10.1038/NCHEM.806

[14] L. H. Renbaum, G. D. Smith, Artifacts in measuring aerosol uptake kinetics: the roles of time, concentration and adsorption. *Atmos. Chem. Phys.* **2011**, *11*, 6881. doi:10.5194/ACP-11-6881-2011

[15] J. D. Smith, J. H. Kroll, C. D. Cappa, D. L. Che, C. L. Liu, M. Ahmed, S. R. Leone, D. R. Worsnop, K. R. Wilson, The heterogeneous reaction of hydroxyl radicals with sub-micron squalane particles: a model system for understanding the oxidative aging of ambient aerosols. *Atmos. Chem. Phys.* **2009**, *9*, 3209. doi:10.5194/ACP-9-3209-2009

[16] J. H. Kroll, J. D. Smith, D. L. Che, S. H. Kessler, D. R. Worsnop, K. R. Wilson, Measurement of fragmentation and functionalization pathways in the heterogeneous oxidation of oxidized organic aerosol. *Phys. Chem. Chem. Phys.* **2009**, *11*, 8005. doi:10.1039/B905289E

[17] D. L. Che, J. D. Smith, S. R. Leone, M. Ahmed, K. R. Wilson, Quantifying the reactive uptake of OH by organic aerosols in a continuous flow stirred tank reactor. *Phys. Chem. Chem. Phys.* **2009**, *11*, 7885. doi:10.1039/B904418C

[18] S. H. Kessler, J. D. Smith, D. L. Che, D. R. Worsnop, K. R. Wilson, J. H. Kroll, Chemical Sinks of organic aerosol: kinetics and products of the heterogeneous oxidation of erythritol and levoglucosan. *Environ. Sci. Technol.* **2010**, *44*, 7005. doi:10.1021/ES101465M

[19] S. H. Kessler, T. Nah, K. E. Daumit, J. D. Smith, S. R. Leone, C. E. Kolb, D. R. Worsnop, K. R. Wilson, J. H. Kroll, OH-initiated heterogeneous aging of highly oxidized organic aerosol. *J. Phys. Chem. A* **2012**. doi:10.1021/JP212131M

[20] R. Chirico, P. F. DeCarlo, M. F. Heringa, T. Tritscher, R. Richter, A. S. H. Prevot, J. Dommen, E. Weingartner, G. Wehrle, M. Gysel, M. Laborde, U. Baltensperger, Impact of aftertreatment devices on primary emissions and secondary organic aerosol formation potential from in-use diesel vehicles: results from smog chamber experiments. *Atmos. Chem. Phys.* **2010**, *10*, 11545. doi:10.5194/ACP-10-11545-2010

[21] S. D. Shah, D. R. Cocker, J. W. Miller, J. M. Norbeck, Emission rates of particulate matter and elemental and organic carbon from in-use diesel engines. *Environ. Sci. Technol.* **2004**, *38*, 2544. doi:10.1021/ES0350583

[22] M. J. Northway, J. T. Jayne, D. W. Toohey, M. R. Canagaratna, A. Trimborn, K. I. Akiyama, A. Shimono, J. L. Jimenez, P. F. DeCarlo, K. R. Wilson, D. R. Worsnop, Demonstration of a VUV lamp photoionization source for improved organic speciation in an aerosol mass spectrometer. *Aerosol Sci. Technol.* **2007**, *41*, 828. doi:10.1080/02786820701496587

[23] A. C. Aiken, P. F. DeCarlo, J. L. Jimenez, Elemental analysis of organic species with electron ionization high-resolution mass spectrometry. *Anal. Chem.* **2007**, *79*, 8350. doi:10.1021/AC071150W

[24] A. C. Aiken, P. F. Decarlo, J. H. Kroll, D. R. Worsnop, J. A. Huffman, K. S. Docherty, I. M. Ulbrich, C. Mohr, J. R. Kimmel, D. Sueper, Y. Sun, Q. Zhang, A. Trimborn, M. Northway, P. J. Ziemann, M. R. Canagaratna, T. B. Onasch, M. R. Alfarra, A. S. H. Prevot, J. Dommen, J. Duplissy, A. Metzger, U. Baltensperger, J. L. Jimenez, O/C and OM/OC ratios of primary, secondary, and ambient organic aerosols with high-resolution time-of-flight aerosol mass spectrometry. *Environ. Sci. Technol.* **2008**, *42*, 4478. doi:10.1021/ES703009Q

[25] E. R. Mysak, K. R. Wilson, M. Jimenez-Cruz, M. Ahmed, T. Baer, Synchrotron radiation based aerosol time-of-flight mass spectrometry for organic constituents. *Anal. Chem.* **2005**, *77*, 5953. doi:10.1021/AC050440E

[26] E. Gloaguen, E. R. Mysak, S. R. Leone, M. Ahmed, K. R. Wilson, Investigating the chemical composition of mixed organic-inorganic particles by 'soft' vacuum ultraviolet photoionization: the reaction of ozone with anthracene on sodium chloride particles. *Int. J. Mass Spectrom.* **2006**, *258*, 74. doi:10.1016/J.IJMS.2006.07.019

[27] S. R. Leone, M. Ahmed, K. R. Wilson, Chemical dynamics, molecular energetics, and kinetics at the synchrotron. *Phys. Chem. Chem. Phys.* **2010**, *12*, 6564. doi:10.1039/C001707H

[28] K. R. Wilson, M. Jimenez-Cruz, C. Nicolas, L. Belau, S. R. Leone, M. Ahmed, Thermal vaporization of biological nanoparticles: fragment-free vacuum ultraviolet photoionization mass spectra of tryptophan, phenylalanine−glycine−glycine, and β-carotene. *J. Phys. Chem. A* **2006**, *110*, 2106. doi:10.1021/JP0543734

[29] P. DeCarlo, J. G. Slowik, D. R. Worsnop, P. Davidovits, J. L. Jimenez, Particle morphology and density characterization by combined mobility and aerodynamic diameter measurements. Part 1: theory. *Aerosol Sci. Technol.* **2004**, *38*, 1185.

[30] J. Duplissy, P. F. DeCarlo, J. Dommen, M. R. Alfarra, A. Metzger, I. Barmpadimos, A. S. H. Prevot, E. Weingartner, T. Tritscher, M. Gysel, A. C. Aiken, J. L. Jimenez, M. R. Canagaratna, D. R. Worsnop, D. R. Collins, J. Tomlinson, U. Baltensperger, Relating hygroscopicity and composition of organic aerosol particulate matter. *Atmos. Chem. Phys.* **2011**, *11*, 1155. doi:10.5194/ACP-11-1155-2011

[31] Q. Zhang, M. R. Alfarra, D. R. Worsnop, J. D. Allan, H. Coe, M. R. Canagaratna, J. L. Jimenez, Deconvolution and quantification of hydrocarbon-like and oxygenated organic aerosols based on aerosol mass spectrometry. *Environ. Sci. Technol.* **2005**, *39*, 4938. doi:10.1021/ES048568L

[32] F. W. McLafferty, F. Turecek, *Interpretation of Mass Spectra*, 4th edn **1994** (University Science Books: Mill Valley, CA).

[33] J. J. Schauer, M. J. Kleeman, G. R. Cass, B. R. Simoneit, Measurement of emissions from air pollution sources. 2. C_1 through C_{30} organic compounds from medium duty diesel trucks. *Environ. Sci. Technol.* **1999**, *33*, 1578. doi:10.1021/ES980081N

[34] N. L. Ng, M. R. Canagaratna, J. L. Jimenez, P. S. Chhabra, J. H. Seinfeld, D. R. Worsnop, Changes in organic aerosol composition with aging inferred from aerosol mass spectra. *Atmos. Chem. Phys.* **2011**, *11*, 6465. doi:10.5194/ACP-11-6465-2011

[35] A. M. Sage, E. A. Weitkamp, A. L. Robinson, N. M. Donahue, Evolving mass spectra of the oxidized component of organic aerosol: results from aerosol mass spectrometer analyses of aged diesel emissions. *Atmos. Chem. Phys. Discuss.* **2007**, *7*, 10065. doi:10.5194/ACPD-7-10065-2007

[36] M. A. Miracolo, A. A. Presto, A. T. Lambe, C. J. Hennigan, N. M. Donahue, J. H. Kroll, D. R. Worsnop, A. L. Robinson, Photooxidation of low-volatility organics found in motor vehicle emissions: production and chemical evolution of organic aerosol mass. *Environ. Sci. Technol.* **2010**, *44*, 1638. doi:10.1021/ES902635C

[37] N. Fuchs, A. Sutugin, *Highly Dispersed Aerosols* **1970** (Butterworth-Heinemann: Newton, MA).

[38] A. T. Lambe, M. A. Miracolo, C. J. Hennigan, A. L. Robinson, N. M. Donahue, Effective rate constants and uptake coefficients for the reactions of organic molecular markers (*n*-alkanes, hopanes, and steranes) in motor oil and diesel primary organic aerosols with hydroxyl radicals. *Environ. Sci. Technol.* **2009**, *43*, 8794. doi:10.1021/ES901745H

[39] C. D. Cappa, D. L. Che, S. H. Kessler, J. H. Kroll, K. R. Wilson, Variations in organic aerosol optical and hygroscopic properties upon heterogeneous OH oxidation. *J. Geophys. Res.–Atmos,* **2011**, *116*, D15204. doi:10.1029/2011JD015918

[40] P. F. DeCarlo, E. J. Dunlea, J. R. Kimmel, A. C. Aiken, D. Sueper, J. Crounse, P. O. Wennberg, L. Emmons, Y. Shinozuka, A. Clarke, J. Zhou, J. Tomlinson, D. R. Collins, D. Knapp, A. J. Weinheimer, D. D. Montzka, T. Campos, J. L. Jimenez, Fast airborne aerosol size and chemistry measurements above Mexico City and Central Mexico during the MILAGRO campaign. *Atmos. Chem. Phys.* **2008**, *8*, 4027. doi:10.5194/ACP-8-4027-2008

[41] A. T. Lambe, T. B. Onasch, D. R. Croasdale, J. P. Wright, A. T. Martin, J. P. Franklin, P. Massoli, J. H. Kroll, M. R. Canagaratna, W. H. Brune, D. R. Worsnop, P. Davidovits, Transitions from functionalization to fragmentation reactions of laboratory secondary organic aerosol (SOA) generated from the OH oxidation of alkane precursors. *Environ. Sci. Technol.* **2012**, *46*, 5430. doi:10.1021/ES300274T

[42] Q. Zhang, D. R. Worsnop, M. R. Canagaratna, J. L. Jimenez, Hydrocarbon-like and oxygenated organic aerosols in Pittsburgh: insights into sources and processes of organic aerosols. *Atmos. Chem. Phys.* **2005**, *5*, 3289. doi:10.5194/ACP-5-3289-2005

[43] A. C. Aiken, D. Salcedo, M. J. Cubison, J. A. Huffman, P. F. DeCarlo, I. M. Ulbrich, K. S. Docherty, D. Sueper, J. R. Kimmel, D. R. Worsnop, A. Trimborn, M. Northway, E. A. Stone, J. J. Schauer, R. M. Volkamer, E. Fortner, B. de Foy, J. Wang, A. Laskin, V. Shutthanandan, J. Zheng, R. Zhang, J. Gaffney, N. A. Marley, G. Paredes-Miranda, W. P. Arnott, L. T. Molina, G. Sosa, J. L. Jimenez, Mexico City aerosol analysis during MILAGRO using high resolution aerosol mass spectrometry at the urban supersite (T0) – Part 1: fine particle composition and organic source apportionment. *Atmos. Chem. Phys.* **2009**, *9*, 6633. doi:10.5194/ACP-9-6633-2009

[44] P. F. DeCarlo, I. M. Ulbrich, J. Crounse, B. de Foy, E. J. Dunlea, A. C. Aiken, D. Knapp, A. J. Weinheimer, T. Campos, P. O. Wennberg, J. L. Jimenez, Investigation of the sources and processing of organic aerosol over the Central Mexican Plateau from aircraft measurements during MILAGRO. *Atmos. Chem. Phys.* **2010**, *10*, 5257. doi:10.5194/ACP-10-5257-2010

[45] C. Mohr, J. A. Huffman, M. J. Cubison, A. C. Aiken, K. S. Docherty, J. R. Kimmel, I. M. Ulbricht, M. Hannigan, J. L. Jimenez, Characterization of primary organic aerosol emissions from meat cooking, trash burning, and motor vehicles with high-resolution aerosol mass spectrometry and comparison with ambient and chamber observations. *Environ. Sci. Technol.* **2009**, *43*, 2443. doi:10.1021/ES8011518

[46] J. A. de Gouw, A. M. Middlebrook, C. Warneke, R. Ahmadov, E. L. Atlas, R. Bahreini, D. R. Blake, C. A. Brock, J. Brioude, D. W. Fahey, F. C. Fehsenfeld, J. S. Holloway, M. Le Henaff, R. A. Lueb, S. A. McKeen, J. F. Meagher, D. M. Murphy, C. Paris, D. D. Parrish, A. E. Perring, I. B. Pollack, A. R. Ravishankara, A. L. Robinson, T. B. Ryerson, J. P. Schwarz, J. R. Spackman, A. Srinivasan, L. A. Watts, Organic aerosol formation downwind from the Deepwater Horizon oil spill. *Science* **2011**, *331*, 1295. doi:10.1126/SCIENCE.1200320